Mon. Not. R. Astron. Soc. **376,** 634–644 (2007) doi:10.1111/j.1365-2966.2007.11499.x

Spectral indices of Galactic radio loops between 1420, 820 and 408 MHz

V. Borka★

Laboratory of Physics (010), Vinca Institute of Nuclear Sciences, PO Box 522, 11001 Belgrade, Serbia

Accepted 2006 December 27. Received 2006 December 17; in original form 2005 December 7

ABSTRACT

In this paper, the average brightness temperatures and surface brightnesses at 1420, 820 and 408 MHz of the six main Galactic radio-continuum loops are derived, as are their radio spectral indices. The temperatures and surface brightnesses of the radio loops are computed using data taken from radio-continuum surveys at 1420, 820 and 408 MHz. We have demonstrated the reality of Loops V and VI and present diagrams of their spectra for the first time. We derived the radio spectral indices of Galactic radio loops from radio surveys at three frequencies (1420, 820 and 408 MHz) and confirm them to be non-thermal sources. Diameters and distances of Loops I–VI were also calculated. The results obtained are in good agreement with current theories of supernova remnant (SNR) evolution and suggest that radio loops may have a SNR origin.

Key words: radiation mechanisms: non-thermal – surveys – ISM: kinematics and dynamics – supernova remnants.

1 INTRODUCTION

The fact that some radio spurs can be joined into small circles is very well known. The sets of spurs which form small circles are called loops. During the early 70s, four major loops were recognized. Their discoveries and studies took place in this order: Loop I (Large, Quigley & Haslam 1962; Haslam, Large & Quigley 1964; Large, Quigley & Haslam 1966; Salter 1970), Loop II (Large et al. 1962; Quigley & Haslam 1965; Salter 1970), Loop III (Quigley & Haslam 1965; Salter 1970) and Loop IV (Large et al. 1966; Salter 1970; Reich & Steffen 1981). Salter in 1970 gave the most precise determination of these circles' parameters, which were later published in Berkhuijsen, Haslam & Salter (1971). The data Salter used were the best available at the time at 408, 404, 240 and 178 MHz. A detailed review of the subject was published by Salter (1983). Milogradov-Turin (1972, 1982) and Milogradov-Turin & Urošević (1997) made an observation that some other spurs could be connected into loops. They proposed Loop V to be formed by negative latitude spurs in Taurus, Pisces and Pegasus and Loop VI to correspond to the weak positive latitudes spurs in Leo and Cancer. Using the survey at 38 MHz by Milogradov-Turin & Smith (1973), they computed parameters of the proposed loops.

In order to study the structure of Galactic radio loop emission, it is necessary to determine their spectral indices. The differential spectral indices of the North Polar Spur (NPS), the spurs in Aquarius, Pegasus and Taurus were derived using data at 1420, 408 and 38 MHz (Milogradov-Turin & Nikolić 1995a,b). The technique used was that of temperature–temperature plots (TT plots). Berkhuijsen (1971) gives indices for the spurs seen on her survey. Milogradov-Turin (1982) derived differential temperature spectral indices between 404 and 38 MHz.

Spectral index variations of the Galactic radio-continuum emission were discussed in several papers. Lawson et al. (1987) have studied these variations across the northern sky between 1420 and 38 MHz and suggested that the obtained values (about 2.5) are mainly due to the effects of Loops I and III. Also, Reich & Reich (1988a) used radio-continuum surveys at 1420 and 408 MHz to calculate a map of spectral indices across the northern sky and found significant variations between 2.3 and 3.0. The steepest spectra corresponded to the NPS and Loop III. The same authors (Reich & Reich 1988b) gave the estimation $\beta > 2.8$ for Loops I and III which are believed to be nearby, very old supernova remnants (SNRs). These estimates were mostly derived using the method of TT plots over areas of the sky where no strong local features are superposed on the general Galactic background. Webster (1974) studied the spectrum of the galactic non-thermal background radiation using observations at 408, 610 and 1407 MHz and found that the mean differential temperature spectral index was close to 2.8.

With the aim of studying spectral indices of the major radio loops, I–IV, as well as of the radio loops V and VI, we used radio-continuum surveys at three frequencies: 1420 MHz (Reich & Reich 1986), 820 MHz (Berkhuijsen 1972), 408 MHz (Haslam et al. 1982) and calculated the corresponding mean temperatures and brightnesses. Knowing three values of brightnesses, the spectral indices could be calculated as coefficients of linear fits to logaritmic temperature versus frequency plots. Until now, there were no generated spectra using mean temperatures for (at least) two different frequencies, as is necessary for forming the simplest linear kind of spectrum. All earlier determinations of the radio loop spectral indices were

★E-mail: vborka@vin.bg.ac.yu

based on TT methods. The reality of Loops I–VI is investigated by comparing the values of their spectral indices with earlier mentioned studies of spectral indices distribution across the northern sky. In addition, diameters and distances of Loops I–VI were calculated using the Σ–D relation for (SNRs) given by Case & Bhattacharya (1998).

2 DATA

The surveys at 1420 MHz (Reich & Reich 1986), 820 MHz (Berkhuijsen 1972) and 408 MHz (Haslam et al. 1982) provided the data base for the recomputing of small circles for the major loops. The data were obtained from the 1420-MHz Stockert survey (Reich & Reich 1986), the 820-MHz Dwingeloo survey (Berkhuijsen 1972) and the 408-MHz all-sky survey (Haslam et al. 1982). The angular resolutions are 35 arcmin and $1^{\circ}.2$ and $0^{\circ}.85$, respectively. The effective sensitivities are about 50 mK $T_{\rm b}$ ($T_{\rm b}$ is for an average brightness temperature) at 1420 MHz, 0.20 K at 820 MHz and about 1.0 K at 408 MHz. These data are available on MPIfR's Survey Sampler ('Max-Planck-Institut für Radioastronomie', Bonn). This is an online service (http://www.mpifr-bonn.mpg.de/survey.html), which allows users to pick a region of the sky and obtain images at a number of wavelengths.

3 ANALYSIS

The 1420, 820 and 408 MHz continuum surveys specified in Section 2 were used to derive brightness temperature versus frequency spectra, and the spectral indices of Loops I–VI were derived from these.

The average brightness temperatures of the loops at the three frequencies were estimated from the survey data. The areas of the loops were divided into different sections (corresponding to spurs), and estimates for these sections were combined. The longitude and latitude ranges which include spurs of the Loops I–VI are given in Table 1. The areas inside the spurs were chosen using the three surveys specified above. Background radiation was subtracted in this way. First, the temperature of the loop plus background was determined. Next, the background alone near the loop was estimated. Finally, we calculated the difference of these values to yield the average temperature of the loop.

Average 1420, 820 and 408 MHz brightness temperatures and surface brightnesses derived assuming the Rayleigh–Jeans approximation to hold are presented in Table 2. Assuming the spectra to have a power-law form

$$T_{\rm b} = K\nu^{-\beta}, \tag{1}$$

we get

$$\log T_{\rm b} = \log K - \beta \log \nu, \tag{2}$$

where β is spectral index and K is a constant. Knowing three values of brightnesses (derived in this paper), we were able to derive spectral indices from fitting equation (2) to the data. The results are given in Table 3.

Temperatures at 1 GHz were calculated by use of the spectral indices

$$T_{1\ \rm GHz}/T_{\nu\ \rm GHz} = (1/\nu)^{-\beta}. \tag{3}$$

We have converted these values that have been extrapolated to 1 GHz into surface brightness and present them in Table 4.

4 METHOD OF CALCULATION

The areas used to represent the individual loops were obtained from the radio-continuum map of Reich & Reich (1986) in such a way that they contain the brightness temperature contours enclosing the spur features that define the loop. The longitude and latitude ranges of each are given in Table 1. Contour lines, which correspond to the minimum and maximum brightness temperatures for each spur, are taken to define their borders. $T_{\rm min}$ is the lower temperature limit between the background and the spur, and $T_{\rm max}$ is the upper temperature limit between the spur and unrelated confusing sources (superposed on the spur and hence requiring elimination from the calculation). In this manner, background radiation was considered as radiation that would exist if there were no spurs. We used averages over the data within these two curves: the contour for $T_{\rm min}$ and the contour for $T_{\rm max}$.

For evaluating brightness temperatures of the background, we used all measured values below $T_{\rm min}$, inside the corresponding intervals of Galactic longitude (l) and Galactic latitude (b), and lying on the outer side of a spur. The value of $T_{\rm b}$ is approximately constant near a spur. For evaluating the brightness temperatures of a loop

Table 1. The Galactic longitude and latitude for spurs belonging to Loops I–VI and the lower and upper temperature limits for these loops.

Label of the loop	l, b intervals for spurs (°)		1420 MHz Temperature limits (K)		820 MHz Temperature limits (K)		408 MHz Temperature limits (K)	
			$T_{\rm min}$	$T_{\rm max}$	$T_{\rm min}$	$T_{\rm max}$	$T_{\rm min}$	$T_{\rm max}$
Loop I	$l = [40, 0]$	$b = [18, 78]$	3.6	4.1	7.8	9.5	30.0	40.0
	$l = [360, 327]$	$b = [67, 78]$						
Loop II	$l = [57, 30]$	$b = [-50, -10]$	3.6	4.2	7.2	9.9	24.0	36.0
	$l = [195, 130]$	$b = [-70, -2]$						
Loop III	$l = [180, 135]$	$b = [2, 50]$	3.4	4.2	6.4	10.0	21.0	38.0
	$l = [135, 110]$	$b = [40, 55]$						
	$l = [110, 70]$	$b = [6, 50]$						
Loop IV	$l = [325, 285]$	$b = [55, 72]$	3.58	4.0	7.45	7.95	27.5	30.0
Loop V	$l = [189, 178]$	$b = [-25, -13]$	3.6	3.8	7.1	7.8	24.0	33.5
	$l = [147, 133]$	$b = [-50, -39]$						
	$l = [90, 80]$	$b = [-39, -24]$						
Loop VI	$l = [215, 205]$	$b = [29, 40]$	3.38	3.58	5.8	6.9	15.0	23.5
	$l = [207, 196]$	$b = [6, 32]$						

Table 2. Temperatures (K) and brightnesses (10^{-22} W m^{-2} Hz^{-1} Sr^{-1}) of the radio loops at 1420, 820 and 408 MHz, respectively.

Label of	1420 MHz		820 MHz		408 MHz	
the loop	Temperature	Brightness	Temperature	Brightness	Temperature	Brightness
Loop I	0.27 ± 0.05	1.69 ± 0.30	1.35 ± 0.20	2.78 ± 0.40	8.4 ± 1.0	4.31 ± 0.50
Loop II	0.22 ± 0.05	1.36 ± 0.30	1.10 ± 0.20	2.26 ± 0.40	8.0 ± 1.0	4.07 ± 0.50
Loop III	0.30 ± 0.05	1.84 ± 0.30	1.39 ± 0.20	2.87 ± 0.40	8.5 ± 1.0	4.34 ± 0.50
Loop IV	0.08 ± 0.05	0.48 ± 0.30	0.53 ± 0.20	1.09 ± 0.40	3.0 ± 1.0	1.52 ± 0.50
Loop V	0.13 ± 0.05	0.80 ± 0.30	0.58 ± 0.20	1.19 ± 0.40	5.6 ± 1.0	2.86 ± 0.50
Loop VI	0.12 ± 0.05	0.71 ± 0.30	0.62 ± 0.20	1.29 ± 0.40	4.3 ± 1.0	2.20 ± 0.50

Table 3. Spectral indices of radio loops, between 1420, 820 and 408 MHz.

Label of the loop	β
Loop I	2.74 ± 0.08
Loop II	2.88 ± 0.03
Loop III	2.68 ± 0.06
Loop IV	2.90 ± 0.28
Loop V	3.03 ± 0.15
Loop VI	2.90 ± 0.09

Table 4. Brightnesses (10^{-22} W m^{-2} Hz^{-1} Sr^{-1}) reduced to 1000 MHz.

Label of the loop	1420 MHz reduced to 1000 MHz	820 MHz reduced to 1000 MHz	408 MHz reduced to 1000 MHz
Loop I	2.19 ± 0.72	2.40 ± 0.47	2.22 ± 0.42
Loop II	1.85 ± 0.45	1.90 ± 0.34	1.85 ± 0.26
Loop III	2.32 ± 0.62	2.50 ± 0.38	2.36 ± 0.40
Loop IV	0.66 ± 0.74	0.91 ± 0.39	0.68 ± 0.42
Loop V	1.15 ± 0.46	0.97 ± 0.34	1.14 ± 0.24
Loop VI	0.98 ± 0.41	1.08 ± 0.34	0.98 ± 0.26

including the background, we used all measured values between $T_{\rm min}$ and $T_{\rm max}$ inside the corresponding regions of l and b. If the value of $T_{\rm min}$ (or $T_{\rm max}$) is changed by a small amount, say approximately $2 \times \Delta T$ (i.e. 0.1 K for 1420 MHz, 0.4 K for 820 MHz and 2 K for 408 MHz), the brightness contours become significantly different. If $T_{\rm min}$ is too small, the area of the spur becomes confused with the background and it becomes obvious that the border has been incorrectly chosen. If $T_{\rm max}$ is too large, the area of the spur includes significant contributions from unrelated confusing sources. Mean brightness temperatures for spurs are found by subtracting the mean values of background brightness temperature from the mean values of the brightness temperature over the areas of the spurs.

We calculated the mean background levels over regions not too far outside the spurs because the loops are moving through regions of the interstellar medium where earlier SNRs are likely to have passed, i.e. through a low-density medium produced by earlier SNRs (or other energetic phenomena) (McKee & Ostriker 1977; Salter 1983).

We used averages over the defined areas and subtracted from these the average values for the background regions obtained as described above.

The areas over which an average brightness temperature is determined at each of the three frequencies are taken to be as similar as possible within the limits of measurement accuracy. Moreover, in some cases (e.g. at 1420 MHz for Loops IV and VI), we used values of $T_{\rm min}$ and $T_{\rm max}$ which are below this limit (see Table 1) in order to make the corresponding areas the most comparable. However, some differences between these areas still remain and we think that the major causes of differing borders between the three frequencies are small random and systematic errors in the calibrated data.

5 RESULTS

The results for the six loops are presented in Tables 2 and 3. Table 2 shows calculated average brightness temperatures and surface brightnesses at 1420, 820 and 408 MHz. These results are in good agreement with results obtained by Berkhuijsen (1973), only that the present results are obtained with more sample points. As one can see from Table 1, the first two regions of Loop V are located inside the area of Loop II. The results corresponding to these two loops, presented in Table 2, are calculated out of their overlapping regions. However, we also performed calculations for complete areas of Loops II and V (including overlapping regions) and obtained practically the same results for Loop II. In the case of the whole Loop V, the results for $T_{\rm b}$ are slightly different from those given in Table 2: 0.14 K at 1420 MHz, 0.51 K at 820 MHz and 5.1 K at 408 MHz. This difference is probably caused by superposition of radiation from both loops. Spectra are presented in Figs 1–6, with Table 3 giving the spectral indices computed for Loops I–VI.

The values of brightness obtained at different frequencies can be intercompared after using the spectral indices of Table 3 to reduce them to the values expected at 1 GHz. The good agreement shown by such an intercomparison is obvious (Table 4).

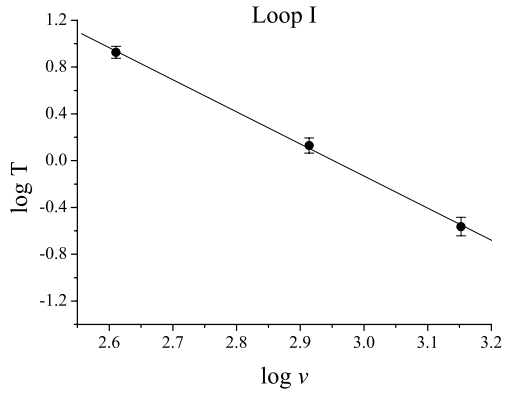

Figure 1. Loop I spectrum: temperature versus frequency for three measurements – at 408, 820 and 1420 MHz. Relative errors of the measurements $\Delta \log T = \frac{\Delta T}{T \ln 10}$ are presented by error bars, where ΔT are the corresponding absolute errors given in Table 2.

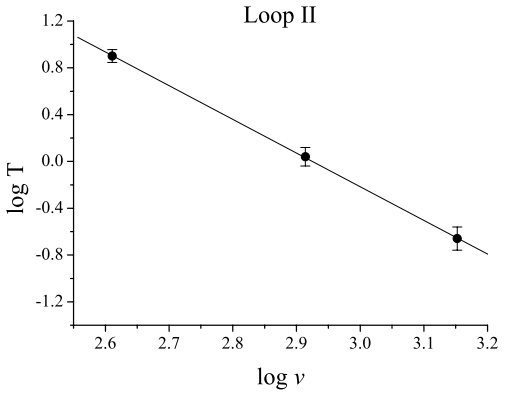

Figure 2. The same as in Fig. 1, but for Loop II.

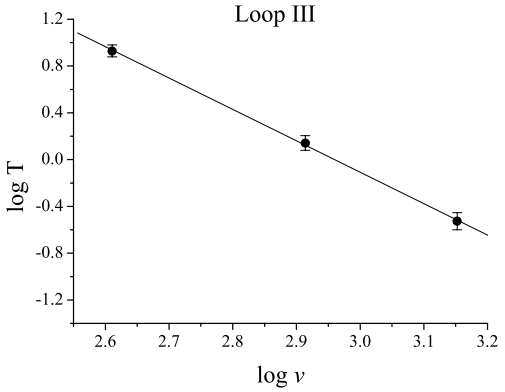

Figure 3. The same as in Fig. 1, but for Loop III.

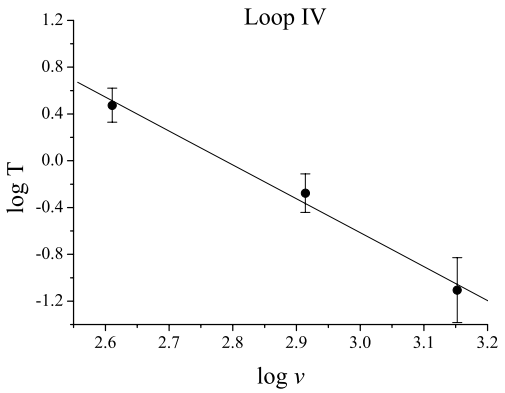

Figure 4. The same as in Fig. 1, but for Loop IV.

When comparing these results with values calculated at other frequencies, and when all results for temperatures are estimated at 1 GHz, the good agreement of these results is obvious (Table 4). The spectra presented in Figs 1–6 are good approximations to simple power-law (straight) spectra between 408, 820 and 1420 MHz, in all but one case, that of Loop IV. The reason for this might be the large relative error of the estimated brightness temperature. A number of effects (Pacholczyk 1970) may play some role in shaping the spectra of the loops at low frequency. From the analysis of differential spectral indices over a range of frequencies, it has been concluded that the spectra of radio loops are curved at low frequencies (Milogradov-Turin & Nikolić 1995a,b). From Figs 1–6, it

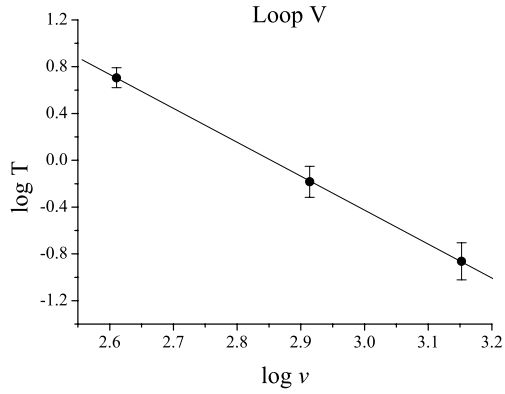

Figure 5. The same as in Fig. 1, but for Loop V.

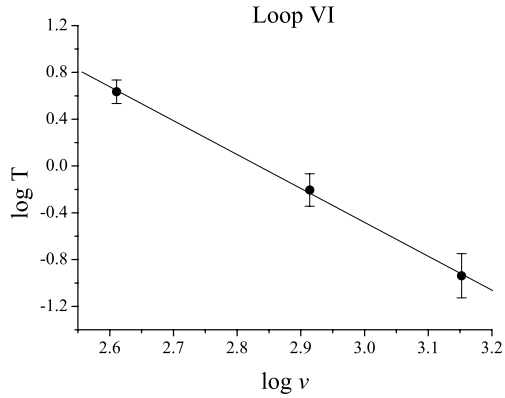

Figure 6. The same as in Fig. 1, but for Loop VI.

can be seen that there is little spectral curvature between 408 and 1420 MHz, and that the data agree well with a linear fit. This is the first spectral investigation of Loops V and VI to be performed in this way. The spectral indices obtained for each of the loops are >2.6, confirming that their radio emissions all have a non-thermal origin.

Assuming that the radio loops are SNRs, they should follow the Σ–D (surface brightness–diameter) relation for SNRs. We have used the relation derived by Case & Bhattacharya (1998) to compute diameters of the Loops I–VI:

$$\Sigma_{1\,\mathrm{GHz}} = 2.82 \times 10^{-17} D^{-2.41} \tag{4}$$

and then for computing distances we use the relation

$$r = D/(2\sin\theta) \tag{5}$$

with angular radii (θ) taken from Milogradov-Turin (1972). The results are given in Table 5. The largest SNRs that Case & Bhattacharya (1998) used to derive their Σ–D relation had diameters of about 100 pc, and 1-GHz brightnesses of about 3×10^{-22} W m^{-2} Hz^{-1} Sr^{-1}. Hence, the application of their relation to the Loops (with $\Sigma_{1\,\mathrm{GHz}} < 2.5 \times 10^{-22}$ W m^{-2} Hz^{-1} Sr^{-1} from Table 4) contains an element of extrapolation.

The smallest values of β occur in the coldest parts of the sky, and the spectral index in the vicinity of Loops I and III is steeper than the spectrum of the background emission. A qualitative explanation of the steepening of the spectrum of emission apparently associated with the Loops I and III has been put forward in terms of diffusive shock-front acceleration (Lawson et al. 1987): there is compression of the interstellar cosmic ray electrons and magnetic field behind a cooling SNR shock front. The resulting map of Reich & Reich

Table 5. Diameters (pc) and distances (pc) of the radio loops derived from the Σ–D relation given by Case & Bhattacharya (1998). Diameters and distances are calculated from brightnesses at 1420, 820 and 408 MHz, respectively, when reduced to 1 GHz. In the last, two columns there are average values of the diameters and distances of the radio loops.

Label of	1420 MHz		820 MHz		408 MHz		average	
the loop	Diameter	Distance	Diameter	Distance	Diameter	Distance	Diameter	Distance
Loop I	132 ± 20	77 ± 14	127 ± 19	74 ± 13	131 ± 20	77 ± 14	130 ± 20	76 ± 14
Loop II	141 ± 22	97 ± 18	140 ± 21	97 ± 18	141 ± 22	98 ± 18	141 ± 22	97 ± 18
Loop III	129 ± 20	115 ± 24	125 ± 19	112 ± 23	128 ± 20	115 ± 23	127 ± 22	114 ± 24
Loop IV	218 ± 33	325 ± 67	190 ± 29	283 ± 58	214 ± 32	319 ± 65	207 ± 32	309 ± 64
Loop V	172 ± 26	91 ± 16	185 ± 28	98 ± 17	173 ± 26	91 ± 16	177 ± 27	93 ± 17
Loop VI	184 ± 28	97 ± 17	177 ± 27	93 ± 16	184 ± 28	97 ± 17	182 ± 28	96 ± 17

(1988a) shows variations of the spectral index between $\beta = 2.3$ and 3.0 and that the areas with steepest spectra are those of the NPS and of Loop III.

When comparing the derived spectral indices with those of the Galactic background (about 2.5 between 408 and 38 MHz, given in Lawson et al. 1987), we can see from Table 3 that these radio loops have steeper, but not much steeper, spectra (about $2.7 < \beta < 2.9$), which provide evidence for the loops being very old SNRs.

The values for the brightness–temperature spectral indices of the loops are rather steep (about $2.7 < \beta < 3.0$). This is at the high end of the spectral index distribution for SNRs in the range $l = [360^\circ, 180^\circ]$ and $D < 36$ pc given by Clark & Caswell (1976), which has a mean T_b spectral index of 2.45. This might be evidence for the steepening of SNR spectra with age, although some authors (see e.g. Clark & Caswell 1976) think there is no indication that the spectral index is correlated with any other features of the SNR.

6 CONCLUSIONS

In this paper, we have calculated the temperatures and surface brightnesses of the Galactic radio loops at 1420, 820 and 408 MHz. We are supposing all radio loops to be SNRs (Berkhuijsen, Haslam & Salter 1970; Berkhuijsen 1971; Shklovskii & Sheffer 1971; Salter 1983). Our results are consistent with the SNR hypothesis and suggest that the radio loops may have a SNR origin. We have used data from the northern part of the radio survey at 1420 MHz (Reich & Reich 1986) and at 820 MHz (Berkhuijsen 1972), and the all-sky survey at 408 MHz (Haslam et al. 1982). Spectra (temperature versus frequency) have been plotted and these are used to determine spectral indices for the main Galactic loops.

The effective sensitivity of the brightness temperatures are 1.0 K for 408 MHz, 0.2 K for 820 MHz and about 50 mK T_b for 1420 MHz. The most precise measurements (the least relative errors) are in case of 1420 MHz, so positions of the brightness temperature contours of the loops are the most realistic for this frequency. Brightnesses of the radio loops at 408 and 820 and 1420 MHz are in good agreement when reduced to 1 GHz.

We have demonstrated the reality of Loops V and VI. We have also calculated the temperatures, surface brightnesses and spectral indices.

The spectral indices that we derived can be compared with values derived by Reich & Reich (1988b) for Loops I and III. They discussed the distribution of spectral indices of the Galactic radio-continuum emission between 1420 and 408 MHz across the northern sky, as well as the global properties of the Galactic spectral index variations. Our results for spectral indices can also be compared with Berkhuijsen (1973) for Loops I–IV. We note that our values for spectral indices are in between the corresponding values for Loops I and III given in Reich & Reich (1988b) and Berkhuijsen (1973).

In this paper, we present the first radio-continuum spectra for the main radio loops, plus Loops V and VI, made using average brightness temperatures at three different frequencies. We find that good linear fits can be made to each of these, supplying accurate spectral indices.

With calculated radio spectral indices, we were able to estimate diameters of these loops and distances to them. That the radio spectra of the loops are fitted rather well by power-low spectra is consistent with a SNR origin for these features.

REFERENCES

Berkhuijsen E. M., 1971, A&A, 14, 359
Berkhuijsen E. M., 1972, A&AS, 5, 263
Berkhuijsen E. M., 1973, A&A, 24, 143
Berkhuijsen E. M., Haslam C. G. T., Salter C. J., 1970, Nat, 225, 364
Berkhuijsen E. M., Haslam C. G. T., Salter C. J., 1971, A&A, 14, 252
Case G. L., Bhattacharya D., 1998, ApJ, 504, 761
Clark D. H., Caswell J. L., 1976, MNRAS, 174, 267
Haslam C. G. T., Large M. I., Quigley M. J. S., 1964, MNRAS, 127, 273
Haslam C. G. T., Salter C. J., Stoffel H., Wilson W. E., 1982, A&AS, 47, 1
Large M. I., Quigley M. J. S., Haslam C. G. T., 1962, MNRAS, 124, 405
Large M. I., Quigley M. J. S., Haslam C. G. T., 1966, MNRAS, 131, 335
Lawson K. D., Mayer C. J., Osborne J. L., Parkinson M. L., 1987, MNRAS, 225, 307
McKee C. F., Ostriker J. P., 1977, ApJ, 218, 148
Milogradov-Turin J., 1972, MSc thesis, Univ. Manchester
Milogradov-Turin J., 1982, PhD thesis, Univ. Belgrade
Milogradov-Turin J., Nikolić S., 1995a, BA Belgrade, 151, 7
Milogradov-Turin J., Nikolić S., 1995b, BA Belgrade, 152, 11
Milogradov-Turin J., Smith F. G., 1973, MNRAS, 161, 269
Milogradov-Turin J., Urošević D., 1997, BA Belgrade, 155, 41
Pacholczyk A. G., 1970, Radio Astrophysics. Freeman & Co., San Francisco
Quigley M. J. S., Haslam C. G. T., 1965, Nat, 208, 741
Reich P., Reich W., 1986, A&AS, 63, 205
Reich P., Reich W., 1988a, A&AS, 74, 7
Reich P., Reich W., 1988b, A&A, 196, 211
Reich W., Steffen P., 1981, A&A, 93, 27
Salter C. J., 1970, PhD thesis, Univ. Manchester
Salter C. J., 1983, BAS India, 11, 1
Shklovskii I. S., Sheffer E. K., 1971, Nat, 231, 173
Webster A. S., 1974, MNRAS, 166, 355

APPENDIX A: THE RADIO LOOPS AND SPURS AT 1420, 820 AND 408 MHz

Fig. A1 shows temperature scales in K, for 1420, 820 and 408 MHz. Figs A2–A7 show Loops I–VI at 1420, 820 and 408 MHz, with two

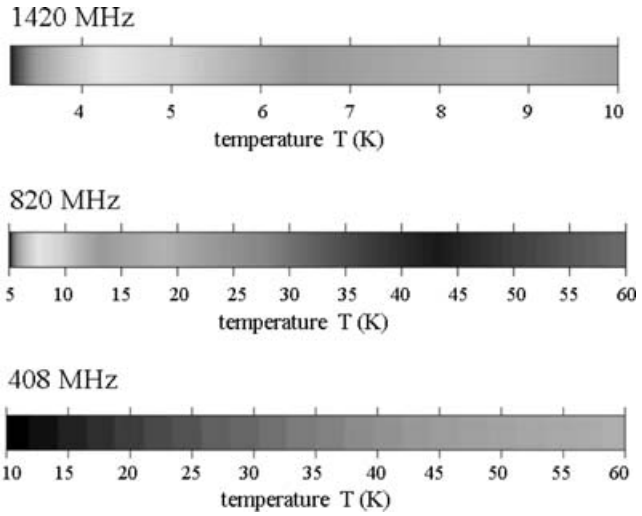

Figure A1. Temperature scales for 1420, 820 and 408 MHz. All are given in K and they are used for all pictures of the radio loops given below.

contours representing the temperatures $T_{\rm min}$ and $T_{\rm max}$ as given in Table 1. Borders between the three frequencies are somewhat different for each loop probably due to small, random and systematic errors in the calibrated data. Also, we suppose there are uncertainties of about 0.1 K in the border of spurs due to measurement errors, and there is a tiny difference in the absorption of radio emission in the interstellar medium at different wavelengths (Pacholczyk 1970).

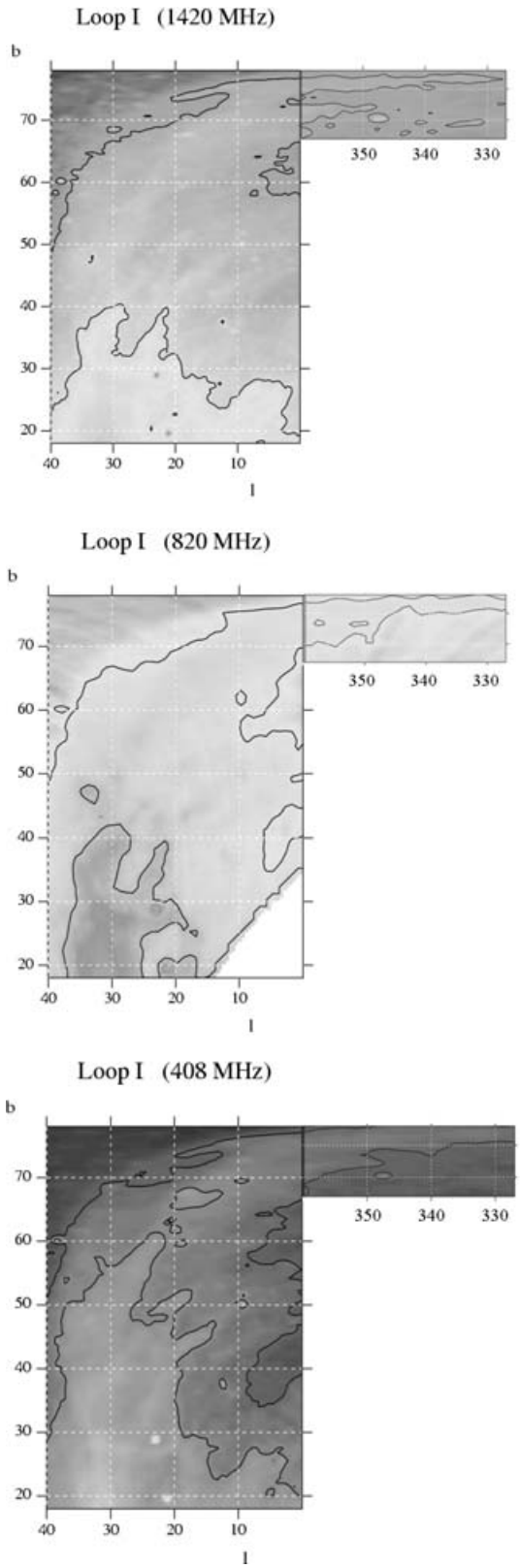

Figure A2. The area of Loop I at 1420, 820 and 408 MHz, showing contours of brightness temperature. This contains the part of the NPS normal to the Galactic plane: $l = [40^\circ, 0^\circ]$; $b = [18^\circ, 78^\circ]$ and its part parallel to the Galactic plane: $l = [360^\circ, 327^\circ]$; $b = [67^\circ, 78^\circ]$. Two contours are plotted, those representing the temperatures $T_{\rm min}$ and $T_{\rm max}$, as given in Table 1.

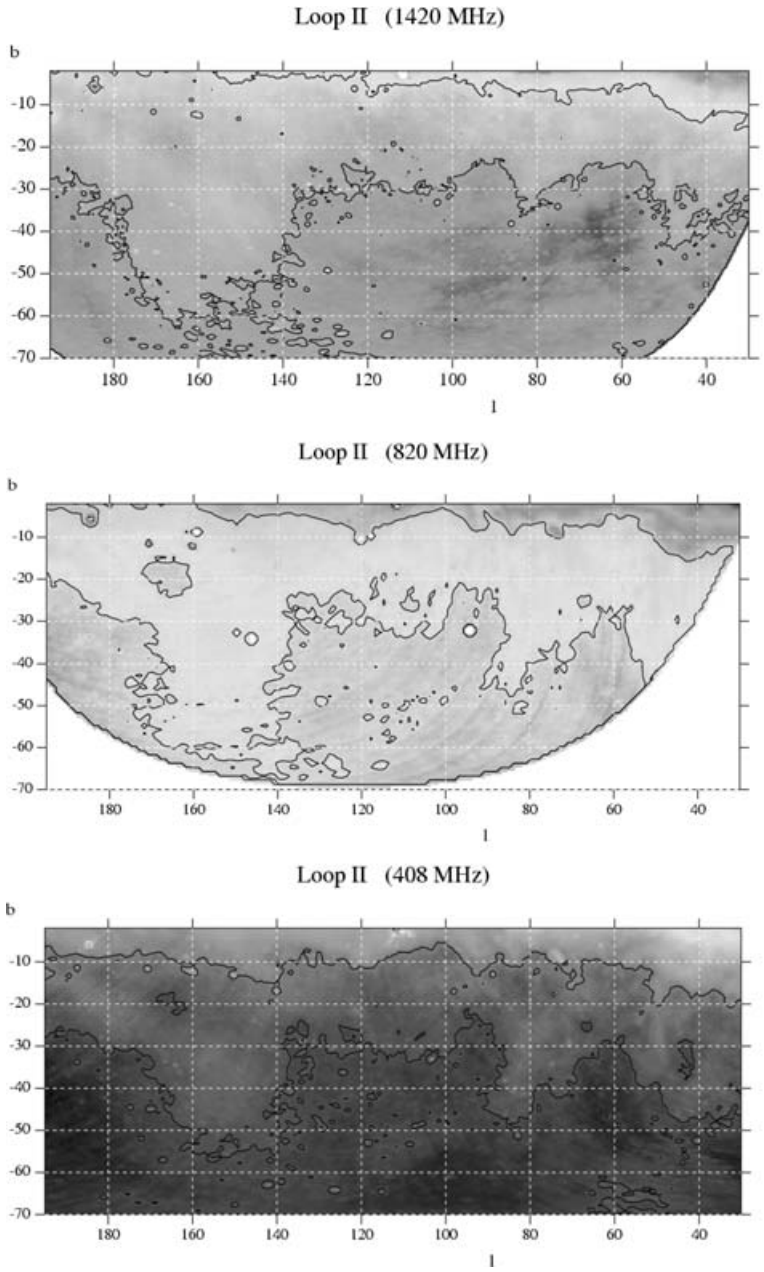

Figure A3. The area of Loop II at 1420, 820 and 408 MHz, showing contours of brightness temperature. The two contours plotted represent the temperatures $T_{\rm min}$ and $T_{\rm max}$, as given in Table 1. White areas in the pictures signify that no data exist there at 1420 and 820 MHz. Spurs belonging to this radio loop have positions: $l = [57^\circ, 30^\circ], b = [-50^\circ, -10^\circ]$ for spur in Aquarius and $l = [195^\circ, 130^\circ], b = [-70^\circ, -2^\circ]$ for spur in Aries.

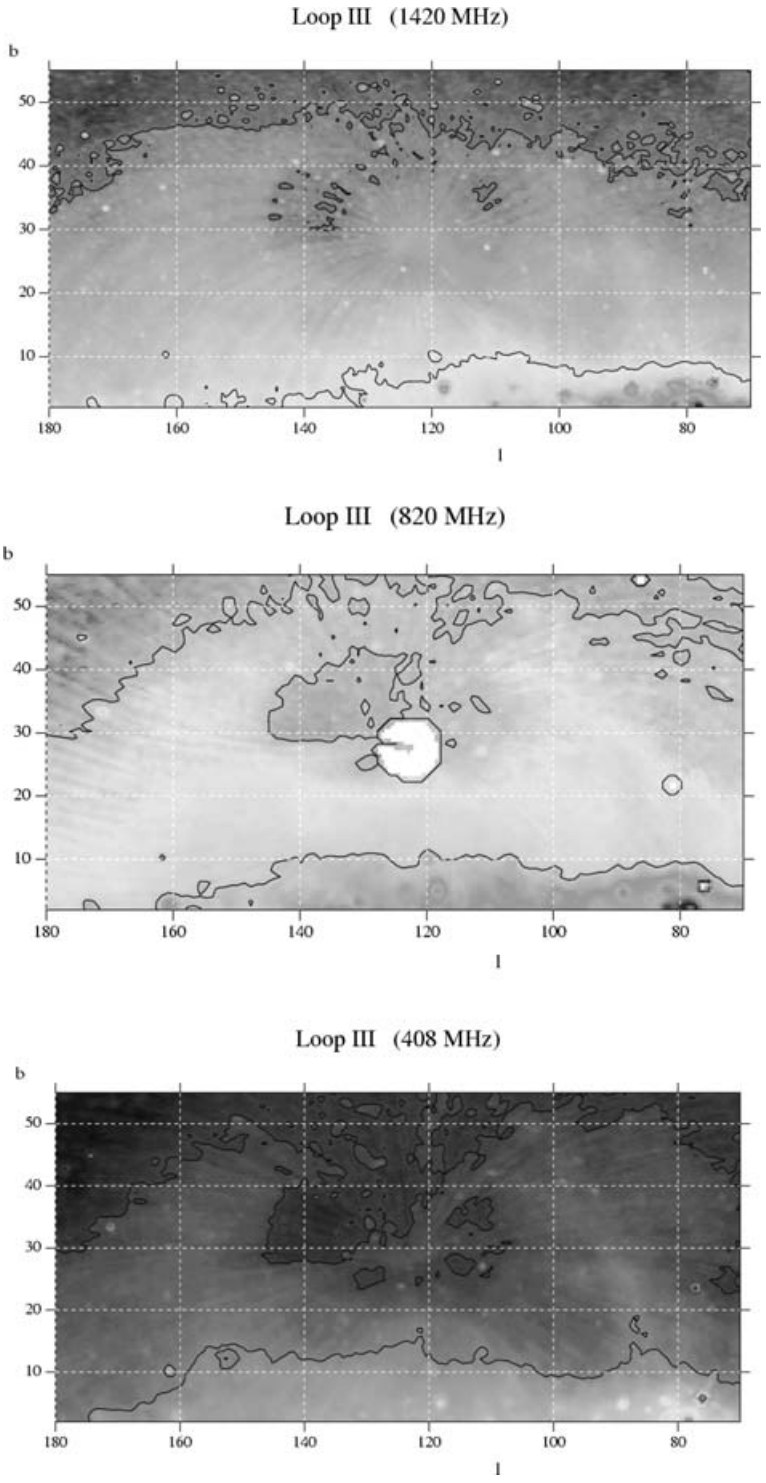

Figure A4. The area of Loop III at 1420, 820 and 408 MHz, showing contours of brightness temperature. The two contours plotted represent the temperatures $T_{\rm min}$ and $T_{\rm max}$, as given in Table 1. The white area in the picture for 820 MHz signifies that no data exist there at that frequency. Spurs belonging to this radio loop have positions: $l = [180^\circ, 135^\circ]$; $b = [2^\circ, 50^\circ]$ and $l = [135^\circ, 110^\circ]$; $b = [40^\circ, 55^\circ]$ for first spur and $l = [110^\circ, 70^\circ]$; $b = [6^\circ, 50^\circ]$ for second one.

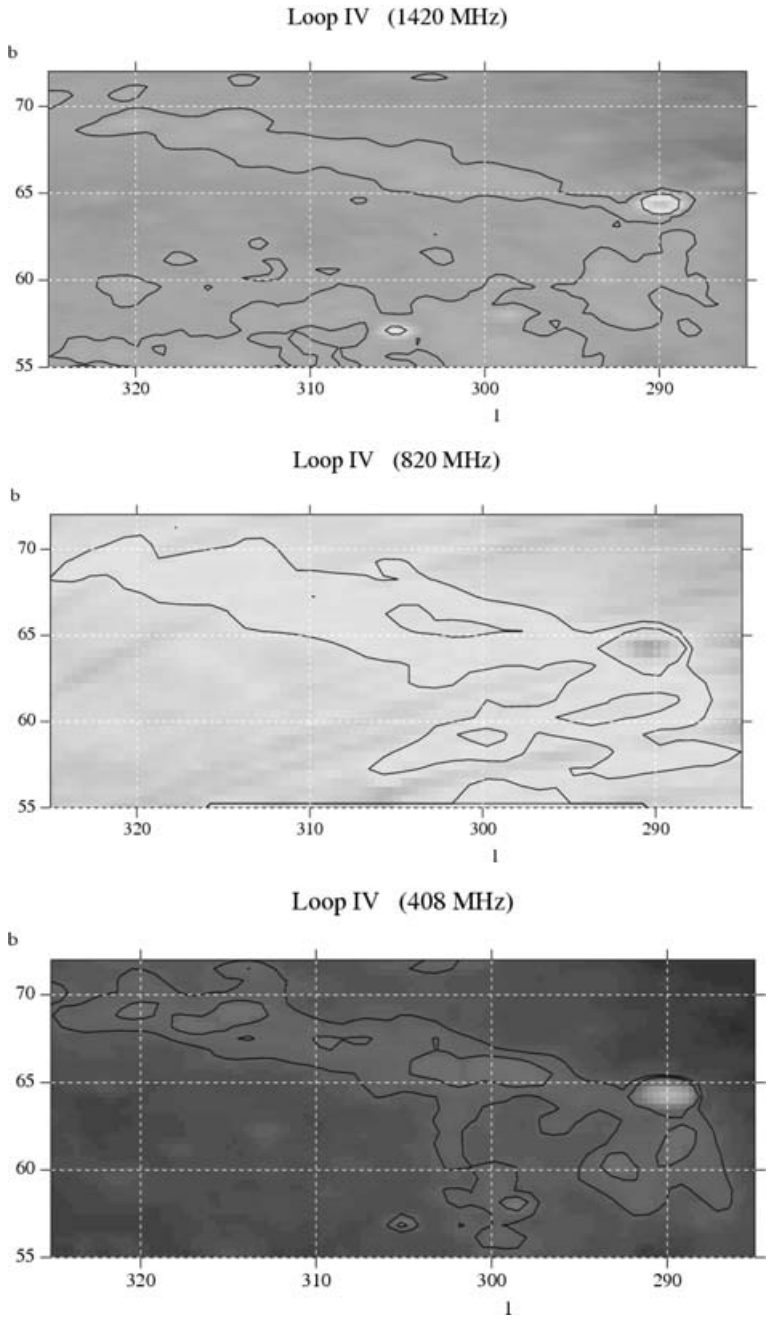

Figure A5. The area of Loop IV at 1420, 820 and 408 MHz, showing contours of brightness temperature. The two contours plotted represent the temperatures $T_{\rm min}$ and $T_{\rm max}$, as given in Table 1. This radio spur has position: $l = [330^\circ, 290^\circ]$; $b = [48^\circ, 70^\circ]$.

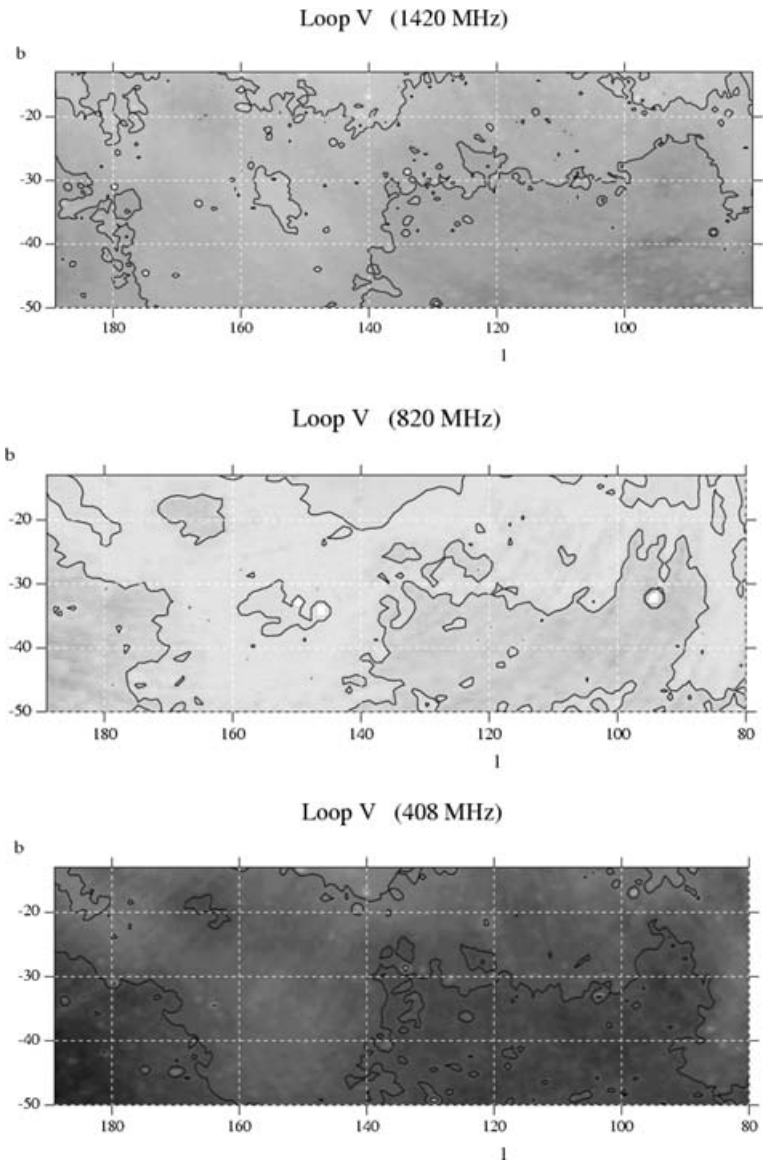

Figure A6. The area of Loop V at 1420, 820 and 408 MHz, showing contours of brightness temperature. The two contours plotted represent the temperatures $T_{\rm min}$ and $T_{\rm max}$, as given in Table 1. Spurs belonging to this radio loop have positions: $l = [189^\circ, 178^\circ]$; $b = [-25^\circ, -13^\circ]$ for the spur in Taurus, $l = [147^\circ, 133^\circ]$; $b = [-50^\circ, -39^\circ]$ for the spur in Pisces and $l = [90^\circ, 80^\circ]$; $b = [-39^\circ, -24^\circ]$ for the spur in Pegasus.

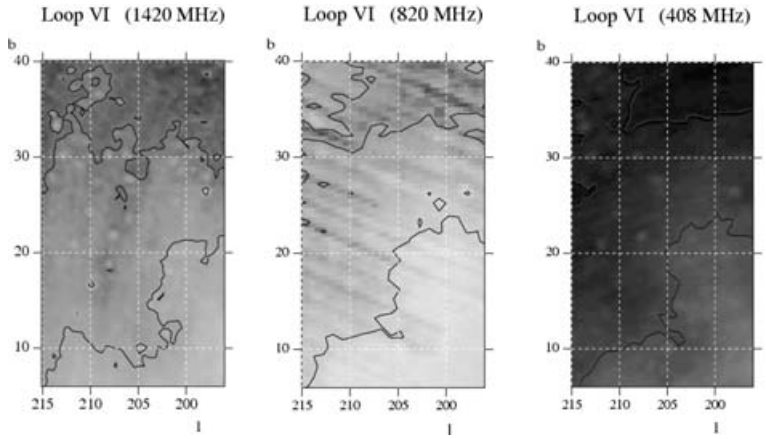

Figure A7. The area of Loop VI at 1420, 820 and 408 MHz, showing contours of brightness temperature. The two contours plotted represent the temperatures $T_{\rm min}$ and $T_{\rm max}$, as given in Table 1. Spurs belonging to this radio loop have positions: $l = [215^\circ, 205^\circ]$; $b = [29^\circ, 40^\circ]$ for the spur in Leo and $l = [207^\circ, 196^\circ]$; $b = [10^\circ, 32^\circ]$ for the spur in Cancer.

This paper has been typeset from a TEX/LATEX file prepared by the author.